

CATHEPSIN INHIBITORS AS POTENT INHIBITORS AGAINST SARS-CoV-2 MAIN PROTEASE. IN SILICO MOLECULAR SCREENING AND TOXICITY PREDICTION

O. SEKIOU¹✉, W. KHERFANE², M. BOUMENDJEL³,
H. CHENIT⁴, A. BENSELHOUB¹✉, S. BELLUCCI⁵

¹Environmental Research Center, Annaba Algeria;

²Laboratory of Geodynamics and Natural Resources, Department of Hydraulics,
Badji Mokhtar Annaba University, Annaba, Algeria;

³Laboratory of Biochemistry and Environmental Toxicology,
Badji Mokhtar Annaba University, Algeria;

⁴National High School of Technology and Engineering (ESTI), Annaba, Algeria;

⁵INFN Frascati National Laboratories, Rome, Italy;

✉e-mail: aissabenselhoub@cre.dz; sekiousmar@yahoo.fr

Received: 05 March 2023; **Revised:** 28 March 2023; **Accepted:** 13 April 2023

Since the emergence of the newly identified Coronavirus SARS-CoV-2, no targeted therapeutic agents for COVID-19 treatment are available, and effective treatment options remain very limited. Successful crystallization of the SARS-CoV-2 main protease (M^{pro} , PDB-ID 6LU7) made possible the research on finding its potential inhibitors for the prevention of virus replication. To conduct molecular docking, we selected ten representatives of the Cathepsin inhibitors family as possible ligands with a high potential of binding the active site of SARS-CoV-2 main protease as a potential target. The results of molecular docking studies revealed that Ligand1 and Ligand2, with vina scores -8.8 and -8.7 kcal/mol for M^{pro} , respectively, were the most effective in binding. In silico prediction of physicochemical and toxicological behavior of assessed ligands approved the possibility of their use in clinical essays against SARS-COVID-19.

Key words: SARS-CoV-2, COVID19, main protease, 6lu7, cathepsin inhibitors, molecular docking, in silico prediction.

Coronavirus disease 2019 (COVID-19) is a viral respiratory disease of zoonotic origin caused by the novel severe acute respiratory syndrome Coronavirus 2 (SARS-CoV-2) [1].

Coronavirus is an RNA virus consisting of positive-sense single-stranded RNA of approximately 27–32 kb [2, 3]. The virus is known to infect a wide range of hosts, including humans, other mammals, and birds [2], causing a wide range of infections, from common cold symptoms to fatal diseases, such as severe respiratory syndrome [4–7]. In addition to pulmonary infection, the virus appears to have manifestations in the central nervous system and heart [8]. Since the emergence of the newly identified Coronavirus (SARS-CoV-2 which cause Corona Virus Disease 2019, COVID-19) in Wuhan, China, the world has experienced an unprecedented wave of pandemic, with 5,666,064 deaths

(01/02/2022) around the world [9]. Almost all countries are affected (216 countries) with 376,478,335 people diagnosed as positive at the same date. A controversial number of vaccines were administrated around the world, with 9,901,135,980 doses [9], but didn't reach the required result. Research for effective drugs is focused on existing molecules already used as drugs in human or animal pharmacopeia, but also on molecules not known for their antiviral effectiveness. The most effective treatments which have given interesting results are based on the use of Chloroquine and Hydroxychloroquine by blocking viral entry into cells and inhibiting glycosylation of host receptors, proteolytic processing, and endosomal acidification [10–14]. Hydroxy-chloroquine and Azithromycin with antiviral molecules such like Lopinavir and Ritonavir are used combined in the Kaletra® [15]. These agents also have immu-

nomodulatory effects by attenuating the production of cytokines and inhibiting autophagy and lysosomal activity in host cells [16]. The pharmacopeia encompasses thousands of molecules that can be tested [17] to limit the replication of the virus and boost immune functions, such as Ivermectin® [18], but the time available means that we have to focus on some of them, of which we already suspect the probable effectiveness against the coronavirus. Jin et al. [19] successfully crystallized the SARS-CoV-2 main protease (M^{pro}), which is a potential drug target. In our present study, we, therefore, focused on known protease inhibitors and we selected Cathepsin inhibitors for their chemical structures with high potential for inhibition of the active site of the M^{pro} main protease of SARS-CoV-2 (M^{pro}), PDB-ID 6LU7 which represents a potential target for the inhibition of SARS-CoV-2 replication. Cathepsins are proteases found in all animals as well as other organisms. There are approximately a dozen members of this family, which are distinguished by their structure, their catalytic mechanism, and which proteins they cleave. Most of the members become activated at the low pH found in lysosomes. Cathepsins have been identified as therapeutic targets in the search for new drugs against a number of human pathologies, including cancer, Alzheimer's, and osteoporosis [20, 21]. Therefore, in our study, the molecular docking will allow us to see and glimpse the possibilities of using the Cathepsins inhibitor family of molecules against the M^{pro} main proteases of the new coronavirus.

Material and Methods

Protein selection and preparation. The 3D structures of all chemical compounds were downloaded from the PubChem database (<https://pubchem.ncbi.nlm.nih.gov/>). The main protease protein targeted was 6lu7 enzyme. Downloaded structures were prepared prior to docking as follows: PyMOL(TM) Molecular Graphics System, version 2.3.0. software (<http://www.pymol.org>) was used to visualize, remove hetatoms and keep only Chain A, then to convert sdf files to pdb format. Hydrogen bond structures were optimized and atoms in missing loops or side chains were added. Water molecules were removed and files were saved in PDB file format.

Ligand preparation. Structures of our ligands were downloaded from PubChem (<https://pubchem.ncbi.nlm.nih.gov/>) and saved in SDF format. Files

were converted from SDF to PDB format using PyMOL.

Molecular docking. To conduct molecular docking, we selected the binding site of inhibitor N3 as a binding cavity. Docking sites targeted for 6LU7 are: $x = -17.497$; $y = 12.937$; $z = 64.063$, at grid spacing of 0.500 Angstrom. Virtual screening was carried out using AutoDock Vina (AutoDock Vina 1.1.2 <https://vina.scripps.edu>) and the best ligand/protein mode was identified based on the binding energy. The scoring function of AutoDockVina is: $C = \sum_i \langle f_{it} | t_j(r_{ij}) \rangle$, where the summation is over all of the pairs of atoms that can move relative to each other, normally excluding 1–4 interactions, i.e. atoms separated by 3 consecutive covalent bonds. Here, each atom i is assigned a type t_i , and a symmetric set of interaction functions $f_{it} | t_j$ of the interatomic distance r_{ij} should be defined [23].

Data. Table 1 shows the PDB ID, resolution and description of COVID-19 main protease selected for this study. Table 2 provides the structure of chosen ligands.

In silico prediction of physicochemical and toxicological behavior of assessed ligands. Physicochemical and toxicological studies were conducted under SwissADME online software and Molinspiration online software. The SMILES structures of ligands were obtained from the PubChem database. The software allows us to compute and predict ADME parameters (Absorption, Distribution, Metabolism & Excretion), pharmacokinetic properties, “druglike” nature and medicinal chemistry friendliness of molecules, but do not predict if a compound is pharmacologically active. This response is estimated by molecular docking.

Simulation of physicochemical and toxicological behavior of our ligands was obtained from SwissADME developed by the Molecular Modeling Group from the Swiss Institute of Bioinformatics (www.swissadme.ch/index.php). The parameters obtained were: molecular weight (g/mol); H-bond donors; H-bond acceptors; lipophilicity Log Po/w; water solubility (Log S); molar refractivity; blood-brain-barrier (BBB) permeability; gastro intestinal (GI) absorption; skin permeation.

Predicted bioactivity parameters were completed from Molinspiration developed by Bratislava University (<https://www.molinspiration.com/>). The parameters obtained were: G Protein-Coupled Receptor(GPCR) ligand; Ion channel modulator;

Table 1. PDB ID, resolution and description of COVID-19 main protease (<https://pubchem.ncbi.nlm.nih.gov>)

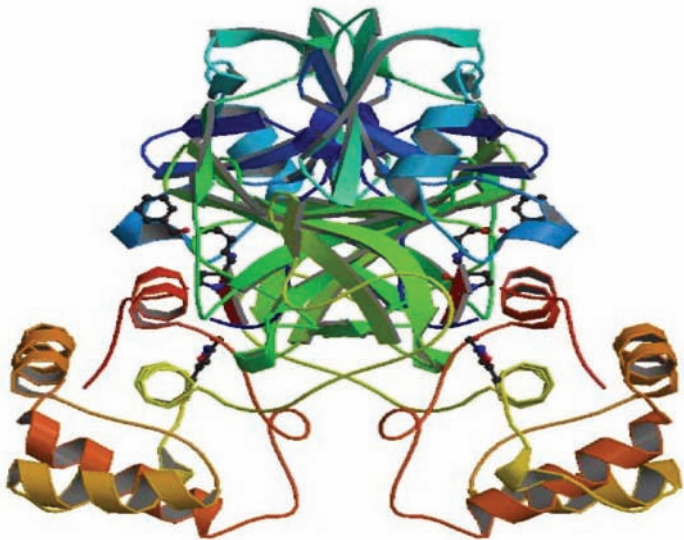
Protein	PDB ID	Resolution (Å)	Structure
COVID-19 main protease	6LU7	2.16 Å	

Table 2. Names and structures of ligands (<https://pubchem.ncbi.nlm.nih.gov>)

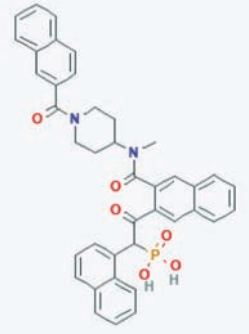
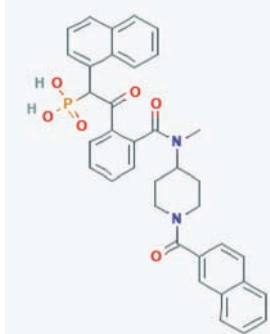
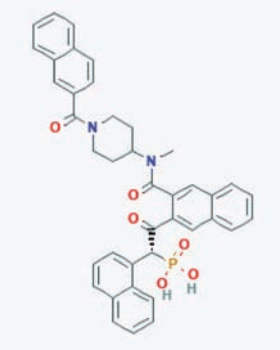
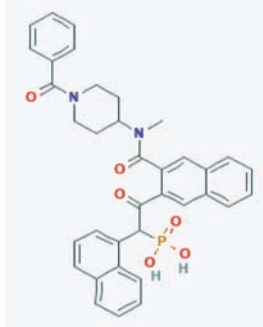
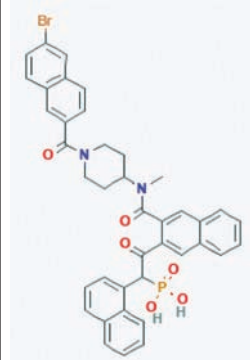
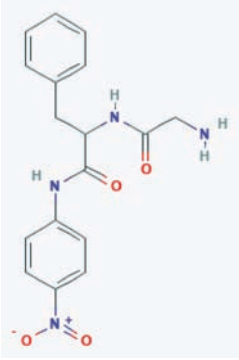
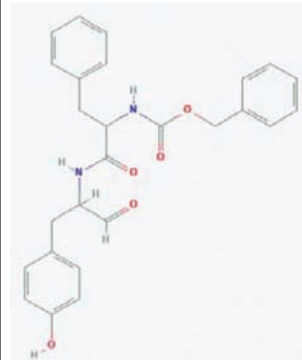
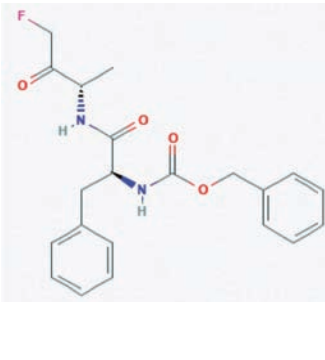
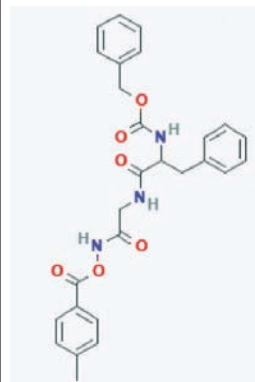
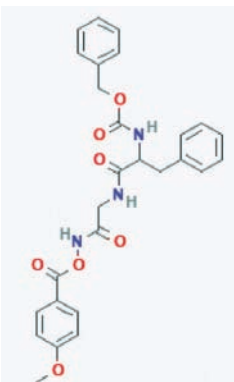
Name of ligand	2D Structure of ligand	Name of ligand	2D Structure of ligand
Ligand 1: JNJ PubChem CID 10311795		Ligand 6: SCHEMBL 4455609 PubChem CID 10145773	
Ligand 2: CILike01 PubChem CID 656932		Ligand 7: Cathepsin G Inhibitor I PubChem CID 9830518	

Table 2. (Continuation)

Name of ligand	2D Structure of ligand	Name of ligand	2D Structure of ligand
Ligand 3: SCHEMBL 1614715 PubChem CID 10190642		Ligand 8: Cathepsin C substrate PubChem CID 3508173	
Ligand 4: Cathepsin D Inhibitor PubChem CID 135340966		Ligand 9: Cathepsin B Inhibitor Z-FA-Fmk PubChem CID 5311161	
Ligand 5: Cathepsin Inhibitor IIF PubChem CID 16760357		Ligand10: CathepsinA Inhibitor PubChem CID 16760358	

Kinase inhibitor; Nuclear receptor ligand; Protease inhibitor; Enzyme inhibitor.

Results and Discussion

Results of binding energies obtained from the docking (AutoDockVina) of COVID-19 main protease (6LU7) active site. The binding energies obtained from the docking (AutoDockVina) of the active site of COVID-19 main protease 6LU7 are presented in Table 3.

Following the docking study, the best scores were obtained with Ligand1 ($-\log S = -8.8$). Described interactions by molecular docking include:

Hydrogen bonds (3); attractive charges (1); Pi-Sulfur interactions (1); Pi-Sigma interactions (1); Pi-Alkyl interactions (2); Pi-Donor Hydrogen bonds (1); and a multitude of Van der Waals interactions. The most important energy was calculated on the basis of Hydrogen bonds. Three H-bonds were established with Glu166 (2.1 Å); His163 (2.1 Å); and Asn142 (2.5 Å) as shown in Table 3 and Fig. 1.

The second best score was obtained with Ligand2 ($-\log S = -8.6$). Described interactions include: Hydrogen bonds (1); attractive charges (1); Pi-Sulfur interactions (1); Pi-Sigma interactions (1); Pi-Alkyl interactions (2); Pi-Donor Hydrogen bonds (1); and

Table 3. Main scores obtained for the ten selected inhibitors and their interacted amino acids

Ligand	Vina score (kcal/mol)	H-Bond	Length	Amino acids residues interaction
Ligand1	-8.8	1	2.1	Glu166
		2	2.1	His163
		3	2.5	Asn142
Ligand2	-8.6	1	2.5	His163
Ligand3	-7.9	1	1.9	Gln189
		2	2.1	Gly143
		3	2.1	Cys145
		4	2.5	Gln189
		5	2.6	Ser144
Ligand4	-7.8	1	2.1	Thr26
		2	2.2	Ser144
		3	2.4	Cys145
		4	2.5	Glu166
		5	2.7	Gly143
		6	2.9	Leu141
Ligand5	-7.8	1	2.2	Cys145
		2	2.3	His163
		3	2.4	Ser144
Ligand6	-7.7	1	1.9	Gln189
		2	2.3	Gly143
		3	2.5	Ser144
		4	2.7	Cys145
Ligand7	-7.5	1	2.0	Gln189
		2	2.3	Gly143
		3	2.5	Ser144
		4	2.6	Cys145
		5	2.7	Gln189
Ligand8	-7.5	1	1.9	Glu166
		2	2.2	Gln189
		3	2.3	Ser144
		4	2.6	Gly143
		5	2.6	Cys145
		6	2.9	Leu141
Ligand9	-6.6	1	2.2	Glu166
		2	2.3	Glu166
		3	2.7	Glu166
Ligand10	-5.0	1	2.2	Lys5
		2	2.9	Lys137

also a multitude of Van der Waals interactions. Only one H-bond was directly established with His163 (2.5 Å) as shown in Table 3 and Fig. 2.

The third score ($-\log S = -7.9$) was obtained by Ligand3. Interactions with this inhibitor exposed the following energy environment: Hydrogen bonds (5); Pi-Sulfur interactions (1); and also a multitude of Van der Waals interactions. The five H-bonds were established with Gln189 (1.9 Å); Gly143 (2.1 Å); Cys145 (2.1 Å); Gln189 (2.5 Å); Ser144 (2.6 Å) as shown on Table 3 and on Fig. 3. The richness of H-bonds of this inhibitor gave it the strong attractivity to the M^{pro} pocket.

The fourth score was due to Ligand4, which is exhibiting a $-\log S = -7.8$. Regarding the difference in the chemical structure, the adopted position in the active site deployed more interactions and a different position including the following low energy interactions: Hydrogen bonds (6); Pi-Sulfur interactions (1); Pi-cation interactions (1); Pi-anion interactions (1); and a multitude of Van der Waals interactions. The five H-bonds were established with Thr26 (2.1 Å); Ser144 (2.2 Å); Cys145 (2.4 Å); Glu166 (2.5 Å); Gly143 (2.7 Å); Leu141 (2.9 Å) as shown on Table 3 and on Fig. 4. The richness of H-bonds of this inhibitor also gave it the strong attractivity to the M^{pro} pocket.

The fifth inhibitor was Ligand5 with $-\log S = -7.8$. The observed interactions were: Hydrogen bonds (3); Pi-donor H-bond interactions (1); Pi-alkyl interactions (1); Carbon H-bond interactions (1); and a multitude of Van der Waals interactions. The three H-bonds were acting with Cys145 (2.2 Å); His163 (2.3 Å); Ser144 (2.4 Å) as shown in Table 3 and Fig. 5.

The sixth molecule exhibiting an interesting score was the Ligand6 with a $-\log S = -7.7$. This inhibitor well fitted into the active enzyme pocket and induced an important variability of low energy bonds including: Hydrogen bonds (4); Pi-Sulfur interactions (1); Pi-Donor Hydrogen bonds (1); with a certain number of Van der Waals interactions. The four H-bonds connected with Gln189 (1.9 Å); Gly143 (2.3 Å); Ser144 (2.5 Å); Cys145 (2.7 Å) as shown in Table 3 and Fig. 6. The low steric blockage of the molecule permitted this inhibitor to display the lowest distance (1.9 Å) with the amino acids into the active site.

The seventh compound was Ligand7 ($-\log S = -7.5$). The predicted interactions for this protease inhibitor were various: Hydrogen bonds (5);

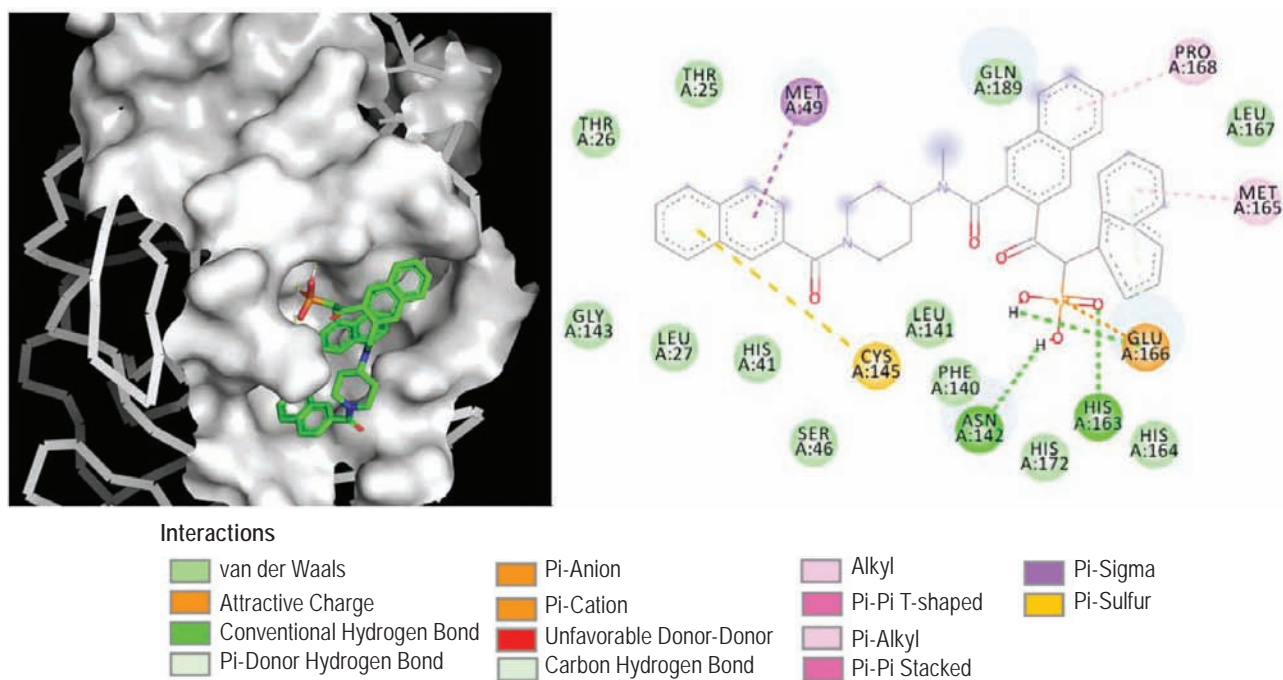


Fig. 1. 3D structure of the active site with Ligand1 ($-\log S = -8.8$) and the amino acids involved in the binding site

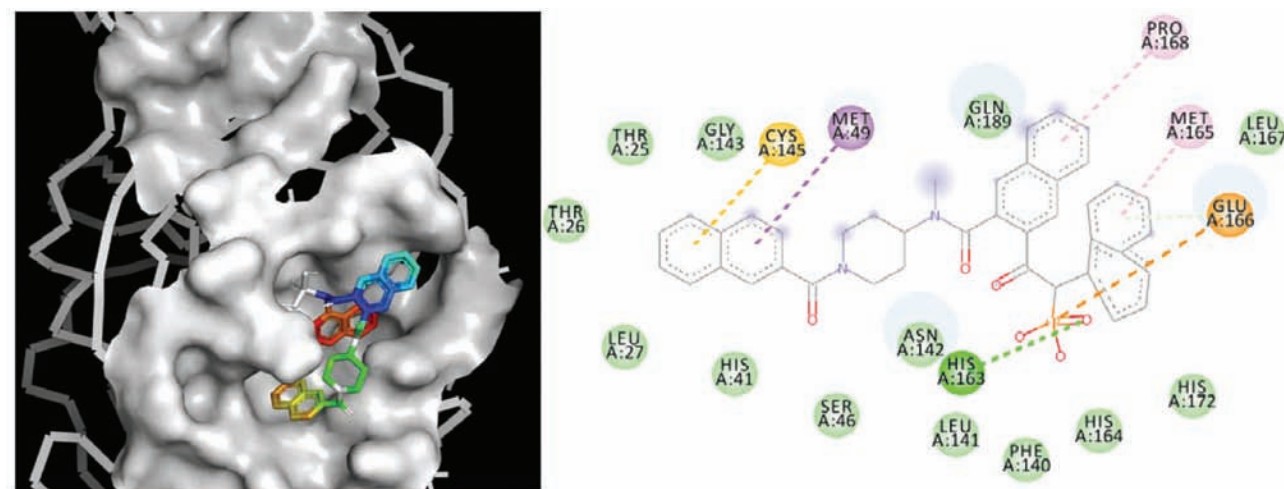


Fig. 2. 3D structure of the active site with Ligand2 ($-\log S = -8.6$) and the amino acids involved in the binding site

Pi-Sulfur interactions (1); Pi-Donor Hydrogen bonds (1); and a significant amount of Van der Waals interactions. These five amino acids were: Gln189 (2.0 Å); Gly143 (2.3 Å); Ser144 (2.5 Å); Cys145 (2.6 Å); and Gln189 (2.7 Å) as shown in Table 3 and Fig 7. We noticed that Ligand7 was able to double interaction with the same amino acid, the Gln189. This was especially due to the phosphoric acid group.

The eighth molecule was Ligand8 ($-\log S = -7.5$). The protease inhibitor was able to establish various interactions: Hydrogen bonds (6); Pi-Sulfur interactions (1); Pi-Donor Hydrogen bonds (1); and a consequent number of Van der Waals interactions. With a huge number of H-bonds (6), this molecule interacted with the following amino acids: Glu166 (1.9 Å); Gln189 (2.2 Å); Ser144 (2.3 Å); Gly143

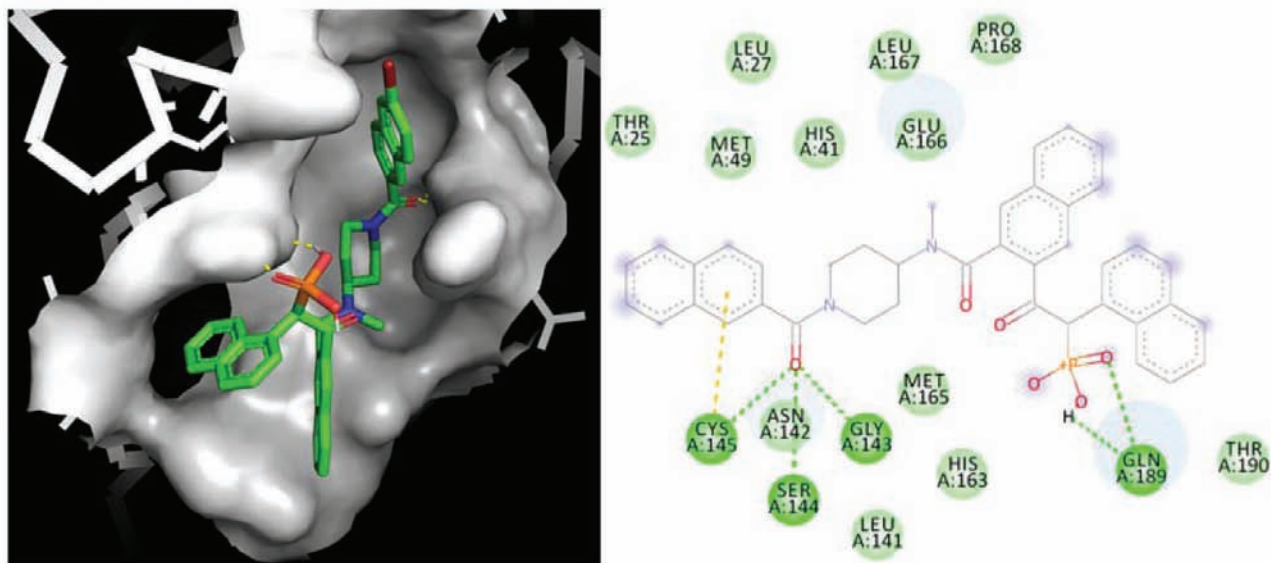


Fig. 3. 3D structure of the active site with Ligand3 ($-\log S = -7.9$) and the amino acids involved in the binding site

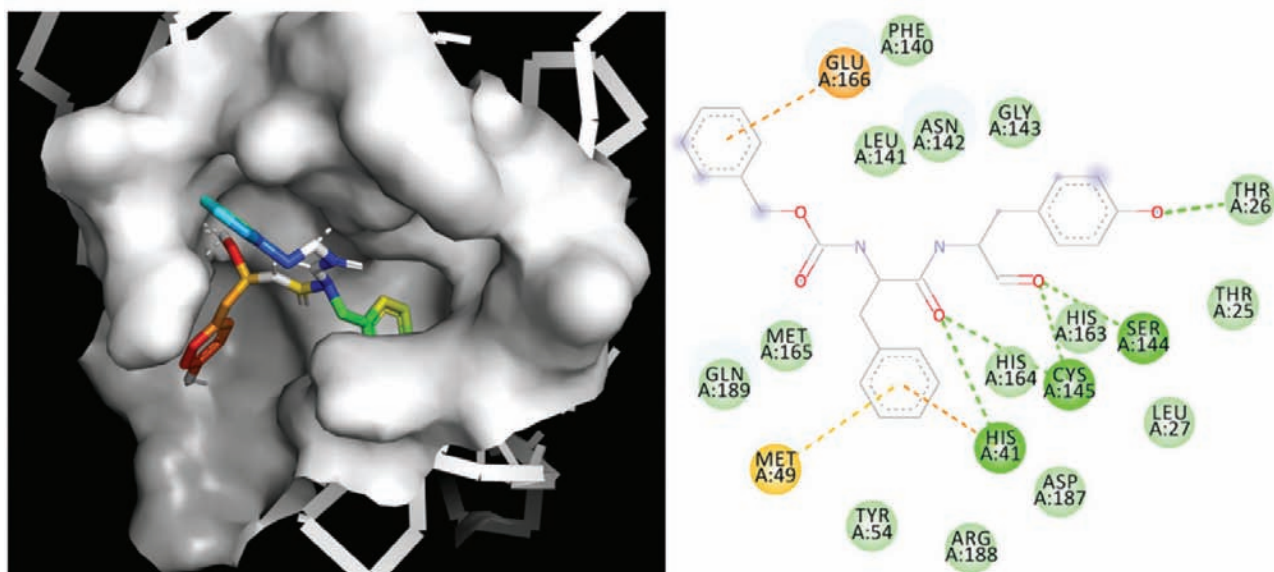


Fig. 4. 3D structure of the active site with Ligand4 ($-\log S = -7.8$) and the amino acids involved in the binding site

(2.6 Å); Cys145 (2.6 Å); and Leu141 (2.9 Å) as shown in Table 3 and Fig. 8.

The ninth compound was Ligand9 with a mean value of -6.6. This special case predicted with only three H-bonds established with the same amino acid (Glu166) is at the limit of acceptable logS values. In addition, it was the only case with unfavorable donor-donor interaction into the M^{pro} pocket. Implied other low-energy interactions were: Pi-Pi T-shaped

interactions (1); Alkyl interactions (1); Pi-Alkyl interactions (1); and common Van der Waals interactions as shown in Table 3 and Fig. 9.

The last inhibitor checked by molecular docking, and also a member of the same family of Cathepsin inhibitors, was Ligand10. Ongoing researches consider molecules with $-\log S < -6$ as inopportune inhibitors. In this case, Ligand10, which exhibited a value of -5.0 (Table 3), can be considered

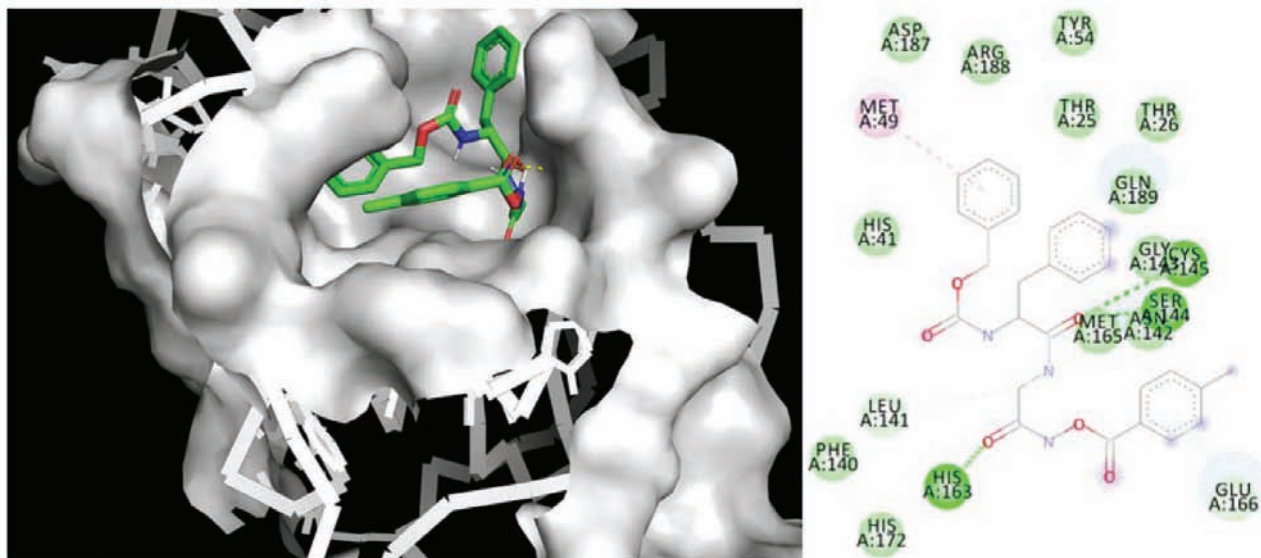


Fig. 5. 3D structure of the active site with Ligand5 ($-\log S = -7.8$) and the amino acids involved in the binding site

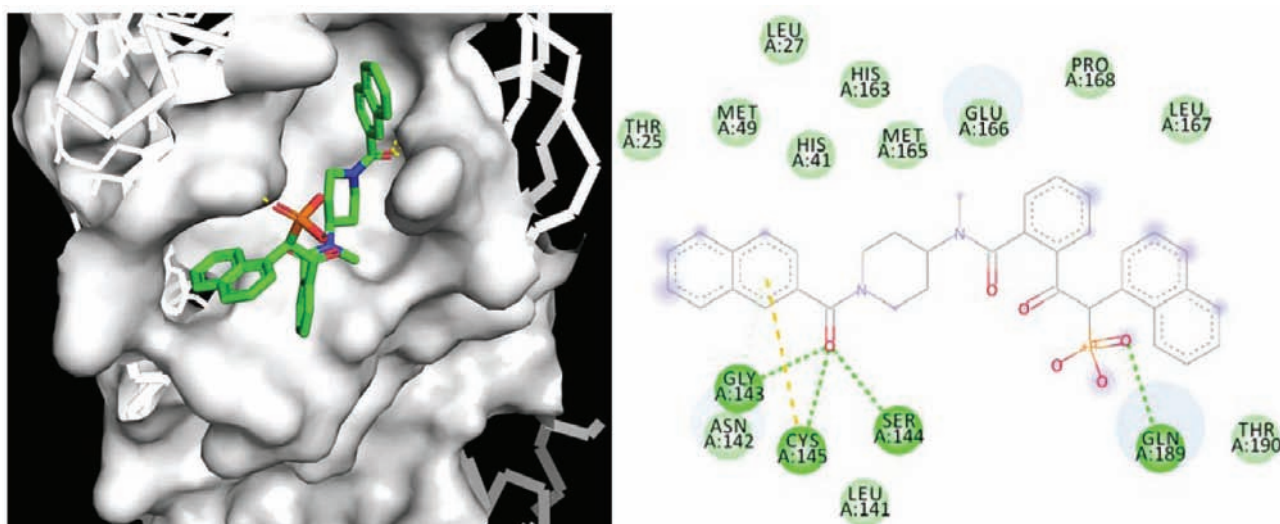


Fig. 6. 3D structure of the active site with Ligand6 ($-\log S = -7.7$) and the amino acids involved in the binding site

as a non-retained compound with low interactions with the M^{pro} pocket. In fact, implied amino acids in both H-bonds were situated outside of the active site of our protease 6lu7 grid.

In silico toxicity study. In the Table 4 we displayed the combined results of SwissADME and Molinspiration predictions. The combined parameters obtained for each checked Cathepsin inhibitor or similar chemical structure were: molecular weight (g/mol); H-bond donors; H-bond acceptors; lipophilicity Log Po/w; water solubility (Log S); molar refractivity; blood-brain-barrier (BBB) permeability;

gastro-intestinal (GI) absorption; skin permeation; G protein-coupled receptor (GPCR) ligand; ion channel modulator; kinase inhibitor; nuclear receptor ligand; protease inhibitor; enzyme inhibitor.

As shown in this table, all molecules, except Ligand4, passed the five rules of Lipinsky, with minor violations. All ligands were of good solubility and no one passed the blood-brain-barrier. Gastro-intestinal (GI) absorption was scored as high for le following ligands: 5; 8; 9 and 10. From these last four molecules, three of them were scored as potent enzyme inhibitors (Ligand5; 9 and 10). No mole-

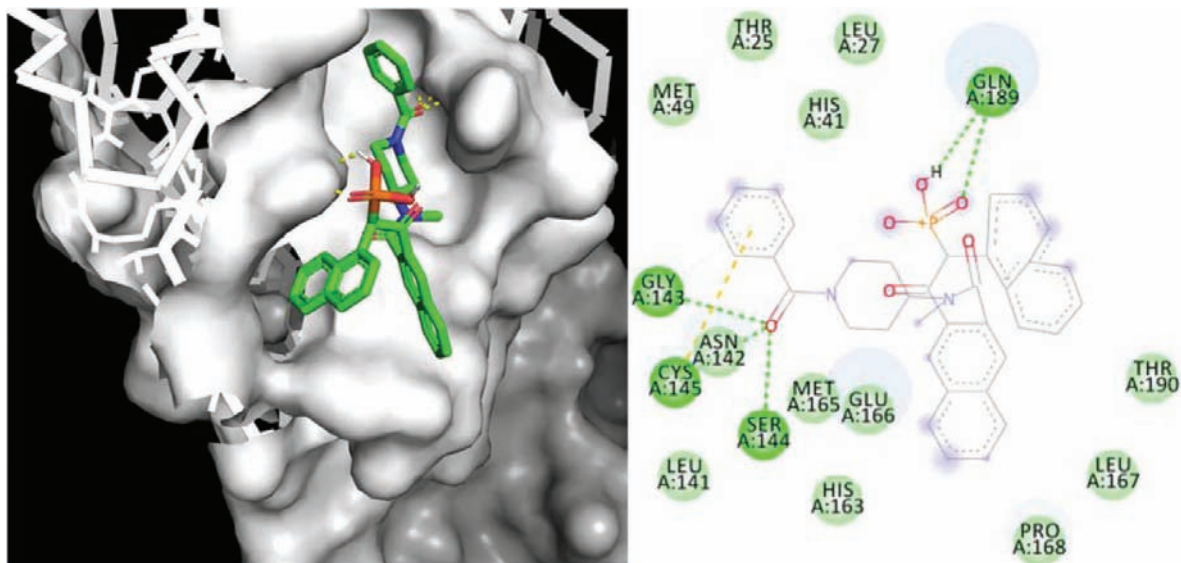


Fig. 7. 3D structure of the active site with Ligand7 ($-\log S = -7.5$) and the amino acids involved in the binding site

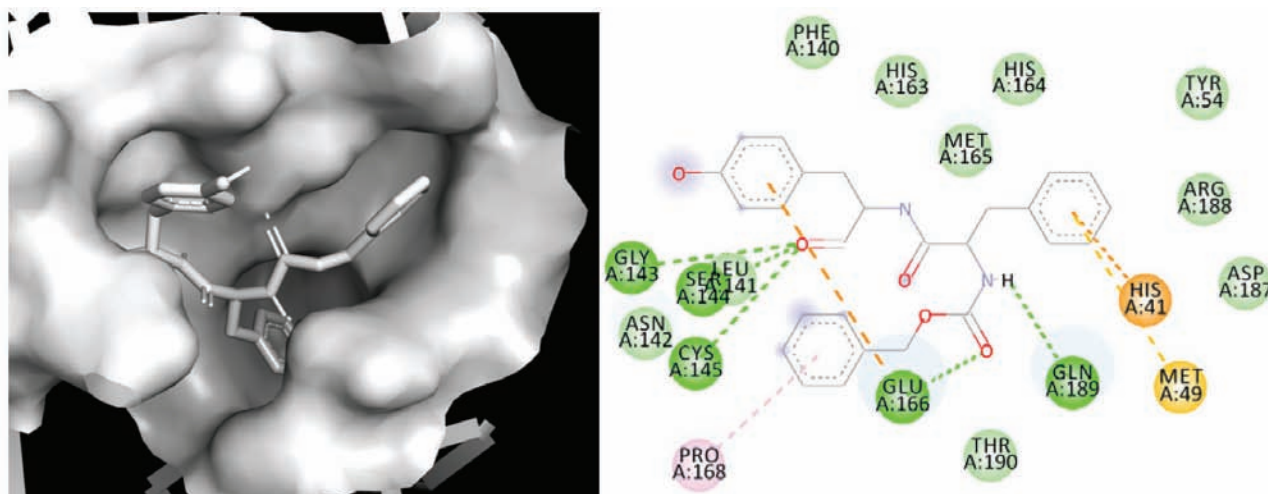


Fig. 8. 3D structure of the active site with Ligand8 ($-\log S = -7.5$) and the amino acids involved in the binding site

cule presented irritant, mutagenic or tumorigenic behavior. These results permit us to conclude their safe-human use.

Conclusion. Research for effective drugs for SARS-CoV-2 Coronavirus focuses on existing molecules used as drugs in human pharmacopeia. Thousands of molecules can be clinically tested, but the available time does not permit it. We focused on some chemical molecules that, we suspected, have probable effectiveness against the Coronavirus. In our present study, we, therefore, focused on known protease inhibitors and selected Cathepsin inhibitors

and similar chemical structures for their high potential of recognizing and inhibiting the active site of the main protease of SARS-CoV-2. *In silico* study allowed us to see and glimpse the possibilities of using this family of molecules against the proteases of the new Coronavirus. Obtained scores ($-\log S$) indicated that nine of the ten checked molecules exhibited an interesting score and that Ligand1 and Ligand2 ranged from -8.8 to -8.7 . All major structures contain aromatic cycles with an important number of H-bonds interactions. *In silico* toxicity study approved the human use of these compounds. We con-

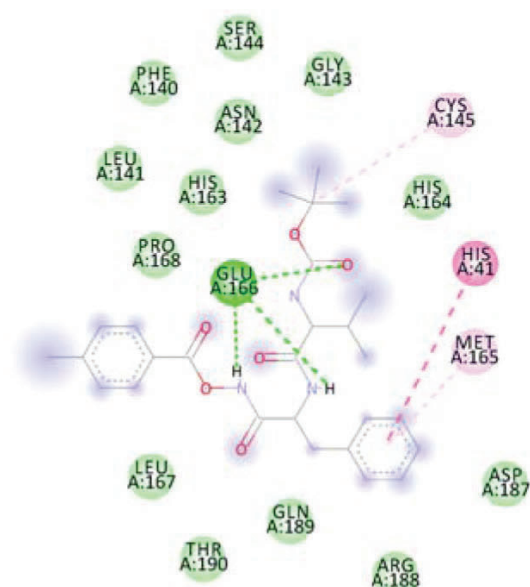
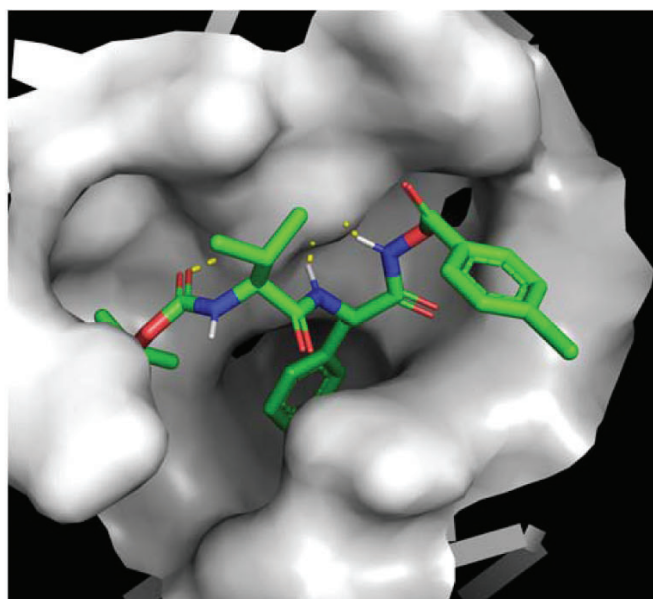


Fig. 9. 3D structure of the active site with Ligand9 ($-\log S = -6.6$) and the amino acids involved in the binding site

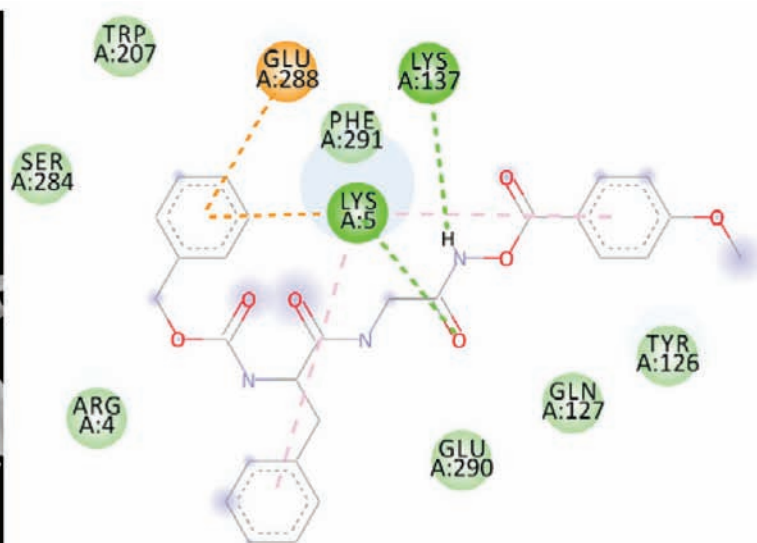
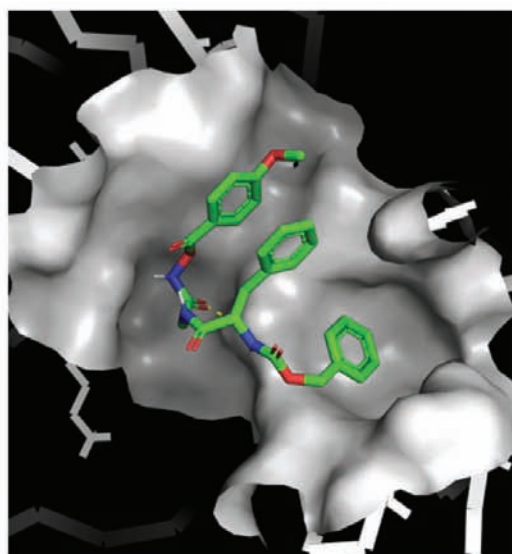


Fig. 10. 3D structure of the active site with Ligand10 ($-\log S = -5.0$) and the amino acids involved in the binding site

clude that this family of chemical structures is very interesting and can be used in clinical essays against the SARS-COVID-19.

Conflict of interest. The authors have completed the Unified Conflicts of Interest form at http://ukr-biochemjournal.org/wp-content/uploads/2018/12/coi_disclosure.pdf and declare no conflict of interest.

Acknowledgments. The present work was supported by DGRSDT (General Directorate of Scientific Research and Technological Development, Algeria) and its FNRSDT project. We especially thank Professor BoudjemaSamraoui for his encouragement and orientations.

Table 4. Prediction of physicochemical and toxicological behavior of assessed ligands

Molecules	Ligand1	Ligand2	Ligand3	Ligand4	Ligand5	Ligand6	Ligand7	Ligand8	Ligand9	Ligand10
PubChem CID	10311795	656932	10190642	135340966	16760357	10145773	9830518	3508173	5311161	16760358
Molecular Weight	670.69	670.7	749.6	NA	489.5 ^o	620.64	620.64	342.35 ^o	386.4 ^o	505.5
H-bond donors	2	2	2	NA	3	2	2	3	2	3
H-bond acceptors	6	6	6	NA	6	6	6	5	5	7
Water solubility	-8.85*	-11.04*	-11.77*	NA	-8.35*	-9.43*	-9.43*	-4.76**	-6.51*	-8.07*
Lipophilicity	5.00	5.00	5.68	NA	3.34	4.15	4.29	0.75	2.69	2.99
Molar Refractivity	196.17	196.17	203.87	NA	130.9 ^{8#}	178.66	178.66	94.19 [#]	102.08 [#]	132.51 [#]
BBB permanent	No	No	No	NA	No	No	No	No	No	No
GI absorption	Low	Low	Low	NA	High	Low	Low	High	High	High
Skin permeation	-6.14	-5.83	-5.82	NA	-6.28	-6.41	-6.41	-7.43	-6.92	-6.66
GPCR ligand	-0.36	-0.36	-0.54	NA	0.16	0.01	0.01	0.09	0.41	0.15
Ion channel modulator	-1.15	-1.15	-1.37	NA	-0.04	-0.56	-0.56	0.00	0.26	-0.08
Nuclear receptor ligand	-0.95	-0.95	-1.19	NA	-0.13	-0.44	-0.44	-0.44	0.16	-0.11
Protease inhibitor	0.18	0.18	0.02	NA	0.59	0.46	0.46	0.28	1.06	0.57
Enzyme inhibitor	-0.52	-0.52	-0.71	NA	0.23	-0.05	-0.05	-0.02	0.28	0.23
Kinase inhibitor	-0.80	-0.80	-0.97	NA	-0.18	-0.30	-0.30	-0.08	-0.05	-0.17
Irritant	No	No	No	No	No	No	No	No	No	No
Mutagenic	No	No	No	No	No	No	No	No	No	No
Tumorigenic	No	No	No	No	No	No	No	No	No	No

Note: NA – Not available

ІНГІБІТОРИ КАТЕПСИНУ ЯК ПОТУЖНІ ІНГІБІТОРИ ОСНОВНОЇ ПРОТЕАЗИ SARS-CoV-2. МОЛЕКУЛЯРНИЙ СКРИНІНГ *IN SILICO* ТА ПРОГНОЗУВАННЯ ТОКСИЧНОСТІ

O. Sekiou¹✉, W. Kherfane², M. Boumendjel³,
H. Cheniti⁴, A. Benselhoub¹✉, S. Bellucci⁵

¹Environmental Research Center, Annaba Algeria;

²Laboratory of Geodynamics and Natural
Resources, Department of Hydraulics, Badji
Mokhtar Annaba University, Annaba, Algeria;

³Laboratory of Biochemistry and
Environmental Toxicology,
Badji Mokhtar Annaba University, Algeria;

⁴National High School of Technology and
Engineering (ESTI), Annaba, Algeria;

⁵INFN Frascati National Laboratories, Rome, Italy;

✉e-mail: aissabenselhoub@cre.dz;
sekiouomar@yahoo.fr

З моменту виявлення нового вірусу, ідентифікованого як коронавірус SARS-CoV-2, не було винайдено таргетних терапевтичних засобів для лікування COVID-19, отже і можливості ефективного лікування залишаються дуже обмеженими. Успішна кристалізація основної протеази SARS-CoV-2 (M^{pro}, PDB-ID 6LU7) сприяла проведенню досліджень у пошуку її потенційних інгібіторів для запобігання реплікації вірусу. Для проведення молекулярного докінгу було обрано десять представників родини інгібіторів катепсину як перспективних лігандів із високим потенціалом зв'язування з активним центром основної протеази SARS-CoV-2 як потенційної мішені. Результати молекулярного докінгу показали, що найефективнішими у зв'язуванні виявилися Ліганд1 та Ліганд2 із показниками ΔG -8,8 та -8,7 ккал/моль для M^{pro}, відповідно. Прогнозування *in silico* фізико-хімічної та токсикологічної поведінки апробованих лігандів підтвердило можливість їх використання в клінічних дослідженнях щодо SARS-COVID-19.

Ключові слова: SARS-CoV-2, COVID-19, основна протеаза, 6lu7, інгібітори катепсину, молекулярний докінг, прогнозування *in silico*.

References

1. Li H, Liu SM, Yu XH, Tang SL, Tang CK. Coronavirus disease 2019 (COVID-19): current status and future perspectives. *Int J Antimicrob Agents*. 2020; 55(5): 105951.
2. Kim JM, Chung YS, Jo HJ, Lee NJ, Kim MS, Woo SH, Park S, Kim JW, Kim HM, Han MG. Identification of Coronavirus Isolated from a Patient in Korea with COVID-19. *Osong Public Health Res Perspect*. 2020; 11(1): 3-7.
3. Elgin TG, Fricke EM, Hernandez Reyes ME, Tsimis ME, Leslein NS, Thomas BA, Sato TS, McNamara PJ. The changing landscape of SARS-CoV-2: Implications for the maternal-infant dyad. *J Neonatal Perinatal Med*. 2020; 13(3): 293-305.
4. Hui DS, Azhar EI, Madani TA, Ntoumi F, Kock R, Dar O, Ippolito G, Mchugh TD, Memish ZA, Drosten C, Zumla A, Petersen E. The continuing 2019-nCoV epidemic threat of novel coronaviruses to global health - The latest 2019 novel coronavirus outbreak in Wuhan, China. *Int J Infect Dis*. 2020; 91: 264-266.
5. Cascella M, Rajnik M, Aleem A, Dulebohn SC, Di Napoli R. Features, Evaluation, and Treatment of Coronavirus (COVID-19). StatPearls [Internet]. Treasure Island (FL): StatPearls Publishing; 2022.
6. Zhai P, Ding Y, Wu X, Long J, Zhong Y, Li Y. The epidemiology, diagnosis and treatment of COVID-19. *Int J Antimicrob Agents*. 2020; 55(5): 105955.
7. Durante-Mangoni E, Andini R, Bertolino L, Mele F, Florio LL, Murino P, Corcione A, Zampino R. Early experience with remdesivir in SARS-CoV-2 pneumonia. *Infection*. 2020; 48(5): 779-782.
8. Sternberg A, McKee DL, Naujokat C. Novel Drugs Targeting the SARS-CoV-2/COVID-19 Machinery. *Curr Top Med Chem*. 2020; 20(16): 1423-1433.
9. World Health Organization. Coronavirus disease (COVID-19) pandemic. Last visit: 02/02/2022. <https://www.who.int/emergencies/diseases/novel-coronavirus-2019>.

10. Sanders JM, Monogue ML, Jodlowski TZ, Cutrell JB. Pharmacologic Treatments for Coronavirus Disease 2019 (COVID-19): A Review. *JAMA*. 2020; 323(18): 1824-1836.
11. Sharma A, Mhatre M, Goldust M, Jindal V, Singla P. The COVID-19 chemoprophylactic conundrum: Are we limiting available resources? *Dermatol Ther*. 2020; 33(4): e13607.
12. Colson P, Rolain JM, Raoult D. Chloroquine for the 2019 novel coronavirus SARS-CoV-2. *Int J Antimicrob Agents*. 2020; 55(3): 105923.
13. Gautret P, Lagier JC, Parola P, Hoang VT, Meddeb L, Sevestre J, Mailhe M, Doudier B, Aubry C, Amrane S, Seng P, Hocquart M, Eldin C, Finance J, Vieira VE, Tissot-Dupont HT, Honoré S, Stein A, Million M, Colson P, La Scola B, Veit V, Jacquier A, Deharo JC, Drancourt M, Fournier PE, Rolain JM, Brouqui P, Raoult D. Clinical and microbiological effect of a combination of hydroxychloroquine and azithromycin in 80 COVID-19 patients with at least a six-day follow up: A pilot observational study. *Travel Med Infect Dis*. 2020; 34: 101663.
14. Colson P, Rolain JM, Lagier JC, Brouqui P, Raoult D. Chloroquine and hydroxychloroquine as available weapons to fight COVID-19. *Int J Antimicrob Agents*. 2020; 55(4): 105932.
15. Cortegiani A, Ingoglia G, Ippolito M, Giarratano A, Einav S. A systematic review on the efficacy and safety of chloroquine for the treatment of COVID-19. *J Crit Care*. 2020; 57: 279-283.
16. Nieuwenhuijs-Moeke GJ, Jainandunsing JS, Struys MMRF. Sevoflurane, a sigh of relief in COVID-19? *Br J Anaesth*. 2020; 125(2): 118-121.
17. Dong L, Hu S, Gao J. Discovering drugs to treat coronavirus disease 2019 (COVID-19). *Drug Discov Ther*. 2020; 14(1): 58-60.
18. Caly L, Druce JD, Catton MG, Jans DA, Wagstaff KM. The FDA-approved drug ivermectin inhibits the replication of SARS-CoV-2 *in vitro*. *Antiviral Res*. 2020; 178: 104787.
19. Jin Z, Du X, Xu Y, Deng Y, Liu M, Zhao Y, Zhang B, Li X, Zhang L, Peng C, Duan Y, Yu J, Wang L, Yang K, Liu F, Jiang R, Yang X, You T, Liu X, Yang X, Bai F, Liu H, Liu X, Guddat LW, Xu W, Xiao G, Qin C, Shi Z, Jiang H, Rao Z, Yang H. Structure of M^{pro} from SARS-CoV-2 and discovery of its inhibitors. *Nature*. 2020 582(7811): 289-293.
20. Vidal-Albalat A, González FV. Natural Products as Cathepsin Inhibitors. *Stud Nat Prod Chem*. 2016; 50: 179-213.
21. Li YY, Fang J, Ao GZ. Cathepsin B and L inhibitors: a patent review (2010 - present). *Expert Opin Ther Pat*. 2017; 27(6): 643-656.
22. Pubchem. Last visit: 07/16/2020. <https://pubchem.ncbi.nlm.nih.gov/>
23. Trott O, Olson AJ. AutoDock Vina: improving the speed and accuracy of docking with a new scoring function, efficient optimization, and multithreading. *J Comput Chem*. 2010; 31(2): 455-461.
24. Swiss Institute of Bioinformatics. Last visit: 07/16/2020. SwissADME. <http://www.swissadme.ch/index.php>
25. Molinspiration. Last visit: 07/16/2020. <https://www.molinspiration.com/>